

# UC Irvine

## UC Irvine Previously Published Works

### Title

de Haas-van Alphen effect and Fermi surface of Nb<sub>3</sub>Sb

### Permalink

<https://escholarship.org/uc/item/6n70v2fp>

### Journal

Physical Review B, 16(4)

### ISSN

2469-9950

### Authors

Arko, AJ  
Fisk, Z  
Mueller, FM

### Publication Date

1977-08-15

### DOI

10.1103/physrevb.16.1387

### Copyright Information

This work is made available under the terms of a Creative Commons Attribution License, available at <https://creativecommons.org/licenses/by/4.0/>

Peer reviewed

## de Haas-van Alphen effect and Fermi surface of Nb<sub>3</sub>Sb

A. J. Arko\*

*Materials Science Division, Argonne National Laboratory, Argonne, Illinois 60439*

Z. Fisk<sup>†‡</sup>

*Institute for Pure and Applied Physical Sciences, University of California at San Diego, La Jolla, California 92093*

F. M. Mueller<sup>§</sup>

*Physics Laboratory and Research Institute for Materials, University of Nijmegen, Toernooiveld, Nijmegen, The Netherlands*

(Received 27 April 1977)

The results of a de Haas-van Alphen investigation of Nb<sub>3</sub>Sb, a compound having the  $\beta$ -W or A-15 structure, are presented. Two families of strong frequencies are consistent with a location of surfaces at the point  $M$  in the simple cubic Brillouin zone. The larger of the two could be an open surface, but the data are inconclusive because of the occurrence of several weak frequency branches. The data are somewhat consistent with the band calculations of Mattheiss for Nb<sub>3</sub>Sn if the Fermi level is shifted.

### I. INTRODUCTION

The properties of compounds based on the A-15 structure have interested both theorists and experimentalists<sup>1</sup> since the first work of Hulm<sup>2</sup> and Matthias.<sup>3</sup> This interest has long focused on the unusually high superconducting critical temperatures of several members of the A-15's, and more recently, on their phononic structure and lattice instabilities.<sup>4</sup>

The electronic band structure has been considered in models of increasing sophistication and complexity.<sup>1,5,6</sup> Yet the difficulty of treating eight atoms per unit cell transition-metal compounds still dictates that the intrinsic accuracy of current band models is far below that of simple, noble, or transition metals. Much of the success in the latter systems can be attributed to the careful interplay between theoretical models and detailed experimental results especially those involving the Fermi surface.

It is likely that the very forces which make the A-15's technologically interesting also dictate that atomically ordered, stoichiometric materials can be prepared only with great difficulty. Of the many examples of A-15's given in the Roberts tables,<sup>7</sup> only a few compounds (e.g., Ti<sub>3</sub>Au, Nb<sub>3</sub>Sb, V<sub>3</sub>Ge, Cr<sub>3</sub>Si) seem to us likely to yield good single crystals with conventional techniques. It is also desirable for observation of the de Haas-van Alphen (dHvA) effect to have the superconducting transition temperatures smaller than about 6 °K in order that  $H_{c2}$  is not too large. We found that Nb<sub>3</sub>Sb yielded single crystals of sufficient quality to yield dHvA signals in a 70-kG field.

The only previous Fermi-surface data on A-15 compounds are the magnetothermal oscillations of

Graebner and Kunzler<sup>8</sup> on V<sub>3</sub>Ge and the positron annihilation data of Berko and Weger.<sup>9</sup> Graebner and Kunzler observed frequencies attributed to three concentric surfaces located at  $M$ . In spite of the differences in materials, some of our data are remarkably similar to theirs. In addition, we see several new pieces of structure.

It is our purpose in measuring the Fermi surface of Nb<sub>3</sub>Sb to provide a benchmark for theorists to utilize in testing and extending their models. We believe that if good agreement can be achieved in the case of low- $T_c$  Nb<sub>3</sub>Sb, then the band models can be reliably applied to the more difficult, complex, and interesting high- $T_c$  systems. The Fermi surface of Nb<sub>3</sub>Sn is, of course, of interest but these measurements need exceptionally high magnetic fields.

Mattheiss has done extensive band calculations for a number of A-15 compounds (including Nb<sub>3</sub>Sn) using the augmented-plane-wave method with linear combination of atomic orbitals fitting.<sup>5</sup> His results cannot be used to study fine details but do serve as a useful guide. Since Sb has only one more electron than Sn and since the lattice parameters of the two compounds differ by less than 1% (see Weger and Goldberg, Ref. 1), we have used a rigid-band shift of his results.

The plan of this paper is as follows: Sec. II describes the methods we have used to grow the single crystals; Sec. III presents our de Haas-van Alphen results and the derived Fermi surface; and Sec. IV gives our conclusions.

### II. SAMPLE PREPARATION

The single crystals of Nb<sub>3</sub>Sb used in this study were prepared by means of an iodine vapor trans-

port technique.<sup>10</sup> A mixture of 0.02-mm 99.8%-Nb foil and 99.99%-Sb ingot was sealed in an evacuated quartz tube of approximately 10 cm length and 1.5 cm diam. The charge mixture was slightly Nb poor—in the proportion  $Nb_{0.7}Sb_{0.3}$ —because we believe that this slight excess of Sb counteracts a small tendency of  $Nb_3Sb$  to be Nb rich. A density of approximately  $2 \text{ mg/cm}^3$  of transporting  $I_2$  was used and an initial 12-h soak at  $900^\circ\text{C}$  pre-reacted the system. Then the quartz tube was placed in a two zone furnace with the charge at the cold end. The warm end was at approximately  $900^\circ\text{C}$  and the cold end at  $800^\circ\text{C}$ . Single-crystal grains of longest dimension 0.5 cm were grown after about 14 d of transport. At  $5^\circ\text{K}$  the lattice constant is  $5.2537 \pm 3 \text{ \AA}$  (kindly measured by A. C. Lawson).

The purity of the single crystals was estimated from measuring the ratio of the resistivity at room temperature to that at  $^4\text{He}$  temperature on some representative samples. Small leads were spot-welded on the crystal. Typical values of resistivities were about  $70 \mu\Omega \text{ cm}$  at room temperature<sup>11</sup> and the resistance ratios were of order 90. (It is likely that some crystal damage occurred in lead placement, so this ratio is probably a lower bound for our samples.) The resistivity ratios of the actual samples used in the experiments described below were not measured. They were selected from each batch on the basis of visual and x-ray examination. The samples were cut to  $1 \text{ mm}^3$  with a spark erosion machine. Surface damage was etched away.

### III. RESULTS AND DISCUSSIONS

The techniques and methodologies utilized in this investigation have been described extensively before.<sup>12</sup> Briefly, the oscillatory component of the magnetic susceptibility was measured by means of the field modulation technique in fields up to 70 kG and temperatures as low as 0.5 K. A dedicated minicomputer was used to perform on-line Fourier transform analysis. We estimate that the angular accuracy of our setting of the external magnetic field relative to the crystallographic axes was about  $1^\circ$  using a rotator with two degrees of freedom.

In Fig. 1 are plotted the extremal cross-sectional areas of the Fermi surface in the (110) and (100) symmetry planes in frequency units. Because of the proximity of several frequency branches, the data are presented as open circles and open diamonds to aid the eye. At the same time, the diamond frequencies were one to two orders of magnitude weaker (in amplitude) than the open circle data. All the data had a signal-to-noise ratio of

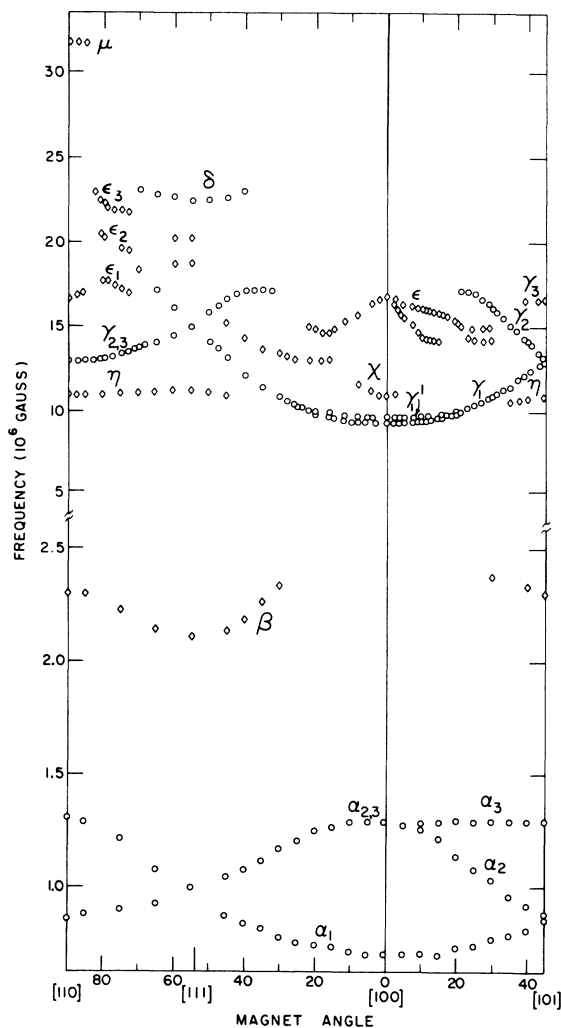


FIG. 1. dHvA frequency spectrum for  $Nb_3Sb$  in the (100) and (110) planes. The division of data into open diamonds and open circles is primarily an aid to the eye in separating the various branches. Simultaneously, the diamond data are much weaker in amplitude than the circle data.

at least 4. This can be seen from the Fourier transform in Fig. 2 for  $H$ ,  $15^\circ$  from [110].

The very strong, low-mass frequencies labeled  $\alpha_i$  can be interpreted in a fairly straightforward manner. They come from a set of closed ellipsoids of revolution centered either at  $X$  or at  $M$  in the simple cubic Brillouin zone with a semimajor axis of  $(0.046 \text{ \AA})^{-1}$  pointing in a  $\langle 100 \rangle$  direction. The semiminor axis has a length of  $(0.086 \text{ \AA})^{-1}$ . A partial Fermi surface is shown in Fig. 3, where these surfaces are labeled  $\alpha$  and are located at the points  $M$  primarily on the basis of the calculations of Mattheiss which indicate that very little band crossing of  $E_F$  is to be expected at  $X$  in nearly all

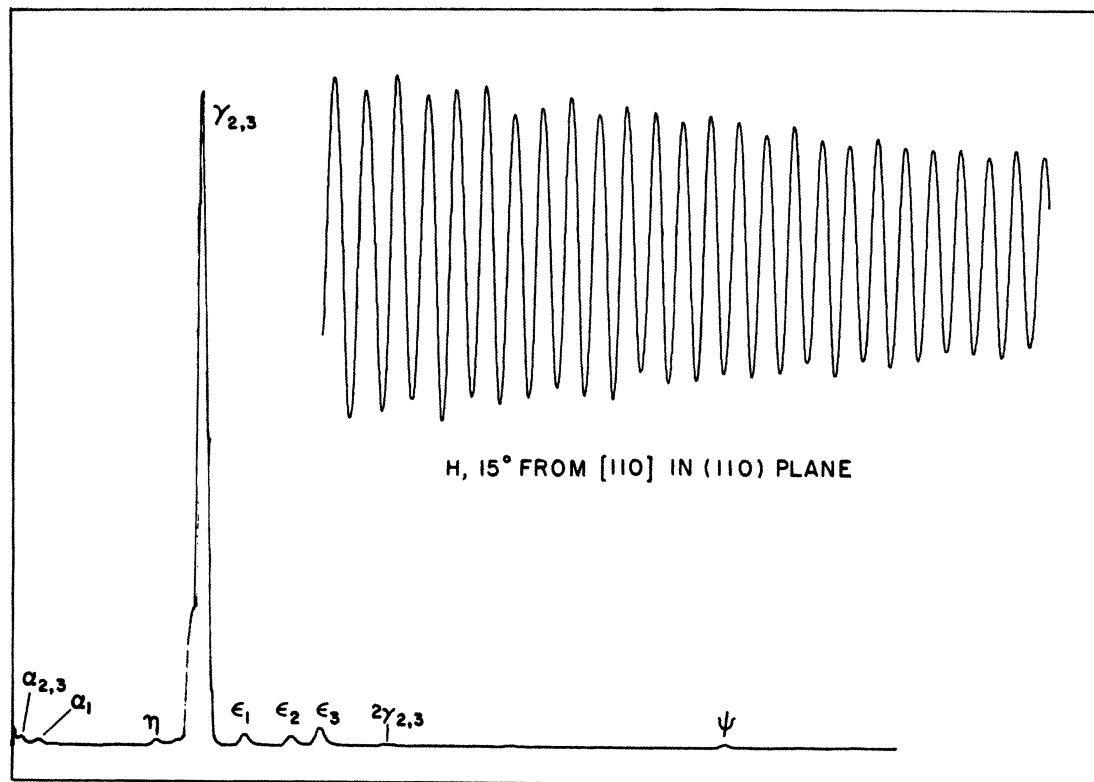


FIG. 2. dHvA oscillations and Fourier transform of data in  $\text{Nb}_3\text{Sb}$  for  $H$ , 15° from [001]. The modulation amplitude was optimized for  $\epsilon_2$ .

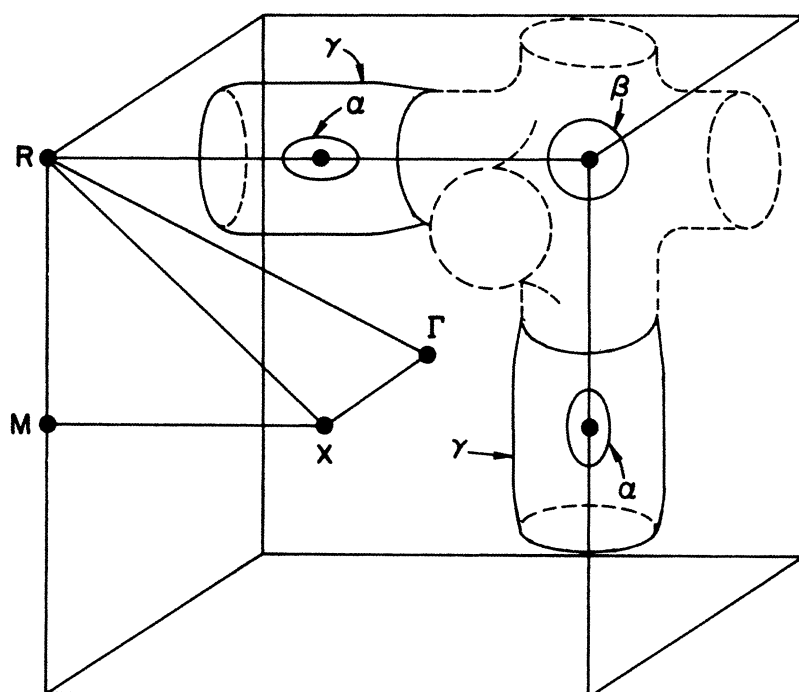


FIG. 3. Partial construction of the proposed Fermi surface of  $\text{Nb}_3\text{Sb}$ . Dashed portions are uncertain and at this time speculative.

TABLE I. Effective masses in Nb<sub>3</sub>Sb.

Frequency	Orientation	$m^*$
$\delta$	[111]	1.58
$\gamma_1$	[111]	1.10
$\gamma_1$	[100]	0.70
$\gamma_1$	[110]	0.89
$\alpha_1$	[111]	0.26

A-15 compounds. Table I gives a list of masses measured at selected field directions.

A second set of strong frequencies,  $\gamma_i$ , also have quite low effective masses (see Table I). At least part of the surface responsible for  $\gamma_i$  has the shape of a cylinder and is again located either at  $X$  or at  $M$ . The known portion of this surface is drawn with solid lines at  $M$  in Fig. 3 and is labeled  $\gamma$ . It is not clear at present whether these cylinders are closed at the ends since the various  $\gamma_i$  branches cut off fairly abruptly and the frequencies labeled  $\epsilon$  are observed in regions where  $\gamma_i$  cut off. It appears that the  $\epsilon$  frequencies are associated in some fashion with the  $\gamma$  surface. Their amplitudes are one to two orders of magnitude lower than  $\gamma_i$ . The cylinders probably have some structure some distance away from the point  $M$  which possibly results in frequencies  $\epsilon$ . The equation for a cylinder is followed by  $\gamma_1$  for about 45° from [100] and then increases slower than a cylinder in the (110) plane. Beyond [111] its amplitude drops drastically and disappears completely within 10° from [111] just as the extremely weak  $\epsilon$  frequencies appear.  $\gamma_1$  apparently reappears within 5° of [011] but the cross-sectional area is considerably smaller than one would expect from a simple extrapolation of  $\gamma_1$  from [111], and its amplitude is no larger than the  $\epsilon$  frequencies. Thus, the identification of this frequency as  $\gamma_1$  in the (110) plane and  $\gamma_3$  in the (100) plane is very tentative. This closed path, presumably around the long portion of the cylinder, has a very narrow angular range as seen from the rapid disappearance of  $\gamma_3$  in the (100) plane.

Ignoring the weak  $\epsilon$  frequencies, it turns out that the  $\gamma_i$  data are remarkably similar to the data of Graebner and Kunzler in V<sub>3</sub>Ge. We do not understand the nature of the structure which interrupts the orbits near the top of the cylindrical surfaces at this time. Indeed it cannot be ruled out that the cylinders contact each other via an  $R$ -centered surface. This speculative topology is shown as the dotted surface in Fig. 3. We will discuss this topology further in connection with frequency  $\delta$ .

Beats exist in  $\gamma_1$  (the second frequency is labeled  $\gamma_1'$ ) for about 20° on either side of [100] in-

dicating a slight dumbbell shape for this surface. In this respect  $\gamma_i$  are different from the V<sub>3</sub>Ge data. The cross-sectional areas at maximum and minimum differ by no more than 3%. Noncentral orbits can be supported by the topology shown in Fig. 3 as drawn, but clearly the  $\gamma$  surface can have a slight depression around the  $M$  point which would also result in noncentral orbits.

Five more weak frequencies,  $\beta$ ,  $\eta$ ,  $\chi$ ,  $\mu$ , and  $\psi$  were observed, all of which are sensitively dependent on sample purity and strain. Frequency  $\psi$  was seen at only two field directions and is not included in Fig. 3. It is included in the Fourier transform of Fig. 2 and has a value of  $48 \times 10^6$  G. Effective masses on these weak frequencies could not be measured because of the weak signals, and in addition, in the case of  $\beta$ , because of interference from the harmonics of  $\alpha_i$ . Indeed,  $\beta$  is very nearly (but not quite) equal to  $(\alpha_1 + \alpha_{2,3})$  for almost the entire range of observation. Frequency  $\beta$  has the symmetry of either  $\Gamma$  or  $R$  and the surface has been placed at  $R$  in Fig. 3. Again, the calculations of Mattheiss for Nb<sub>3</sub>Sn show  $M$  and  $R$  as the most likely locations for pieces of the Fermi surface for  $E_F$  above  $\approx 0.05$  Ry (see Fig. 4). It is assumed that  $\beta$  is a closed surface and that the incomplete range of observation is due to a large effective mass. Clearly, though, this need not be the case. It is possible that  $\beta$  is due to the above-mentioned structure on the  $\gamma$  surface. Similar arguments hold for frequency  $\eta$ ; i.e., it could be a surface centered at  $R$ . Frequencies  $\chi$ ,  $\mu$ , and  $\psi$  were observed over too short an angular range to draw any conclusions.

A somewhat stronger frequency,  $\delta$ , is observed only near [111] and is open to several interpretations. One is that it is associated with a closed piece of Fermi surface centered at  $R$ . The short

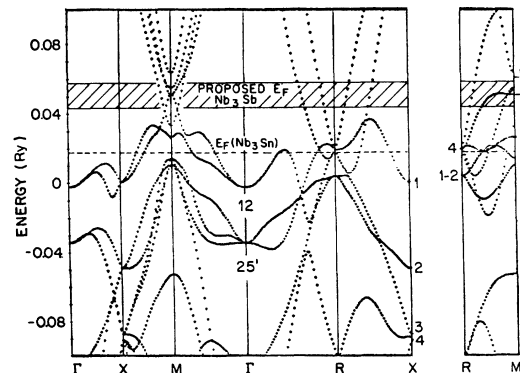


FIG. 4. Nb<sub>3</sub>Sn bands after Mattheiss (Ref. 5). The proposed Fermi level for Nb<sub>3</sub>Sb should lie in the shaded region.

angular range of observation must then be attributed to large effective masses and/or large Dingle temperatures for this surface. With a measured mass of only 1.58 at [111] however, this interpretation seems improbable. Moreover, it does not seem likely that large masses will be obtained from Mattheiss' calculations for bands around  $R$ , even allowing for enhancements.

A second interpretation is that  $\delta$  is a neck orbit of a very large open piece of Fermi surface with  $\langle 111 \rangle$ -directed necks (similar to the Cu Fermi surface). However, no additional frequencies were observed<sup>13</sup> around [100] even at 130 kG.

A third and more plausible interpretation is that the surfaces labeled  $\gamma$  are connected in some fashion to a surface centered at the  $R$  point (dotted portion in Fig. 3) so that the cylindrical  $\gamma$  surfaces become  $\langle 100 \rangle$ -directed necks. The necks then allow closed orbits only near the [111] field direction on the  $R$ -centered surface. Such a topology however would support open orbits. A preliminary magnetoresistance experiment by the authors failed to show clear evidence of  $\langle 100 \rangle$ -directed open orbits. Furthermore, a large hole orbit ( $\approx 90 \times 10^6$  G) would be expected for  $H$  along [100] and was not observed. Additional magnetoresistance experiments and work at higher fields are planned to clear up these points.

It is interesting to note that one of the surfaces obtained from Mattheiss' Nb<sub>3</sub>Sn bands with  $E_F$  placed at  $\approx 0.055$  Ry is a surface at  $R$  joined by cylindrical arms in the  $R-M$  direction. Clearly this type of surface is consistent with the above configuration used to explain the  $\gamma$  and  $\delta$  frequencies.

#### IV. CONCLUSIONS

We have used the band-structure calculations of Mattheiss on a scale of accuracy which is greater

than he might wish. To reflect this we have given the proposed level of  $E_F$  for Nb<sub>3</sub>Sn as the broadened band in Fig. 4. Within such a region, there is fairly good agreement with our data. We wish to make some general observations: (i) A simple addition of two electrons per unit cell raises  $E_F$  to  $\approx 0.035$  Ry, but does not bring it into the region of low density of states needed for Nb<sub>3</sub>Sb. An  $E_F$  of  $\approx 0.055$  Ry is more appropriate. (ii) In the low density of states region above  $E_F$  ( $\approx 0.05$  Ry) the Nb<sub>3</sub>Sn bands (and  $A-15$  bands in general) predict constant energy surfaces only around the points  $M$  and  $R$  consistent with our observations. (iii) Near  $E_F \approx 0.05$  Ry several bands are degenerate or nearly degenerate. Should this prove also to be the case in Nb<sub>3</sub>Sb, one would expect the possibility of magnetic breakdown. Perhaps frequencies  $\epsilon$  can be explained in this manner. Experiments along this line are in progress.

The positron annihilation experiments of Berko and Weger<sup>9</sup> and the band models of Weger and Barak,<sup>14</sup> and Arbman,<sup>15</sup> the resistivity experiments of Fisk and Webb,<sup>11</sup> and other related work,<sup>4</sup> have all invoked complex Fermi surfaces as explanations of behavior of  $A-15$  materials. This together with the yet unexplained  $\beta$ ,  $\epsilon$ ,  $\eta$ ,  $\chi$ ,  $\mu$ , and  $\psi$  frequencies leads us to conclude that our data and proposed Fermi surface are as yet incomplete. Additional work at much higher fields seems warranted. We present our results here because we believe that even in an incomplete form they will serve as a stimulus to others.

#### ACKNOWLEDGMENTS

We wish to thank D. D. Koelling, J. B. Ketterson, G. W. Crabtree, and S. D. Bader for many useful discussions, and to J. F. Barhorst for technical assistance.

\*Work supported by U. S. ERDA.

†Supported by U.S. AFOSR under Contract No. F 49620-77-C-0009.

‡Supported by NSF under Grant No. DMR 75-04019.

§Supported as part of the research program of the "Stichting voor Fundamenteel Onderzoek der Materie" (FOM) with financial support from the "Nederlandse Organisatie voor Zuiver Wetenschappelijk Onderzoek" (ZWO).

<sup>1</sup>For a review, see (a) L. R. Testardi, in *Physical Acoustics*, edited by W. P. Mason and R. N. Thurston (Academic, New York, 1973), Vol. 10; or (b) M. Weger and I. B. Goldberg, in *Solid State Physics*, edited by H. Ehrenreich, F. Seitz, and D. Turnbull (Academic, New York, 1973), Vol. 28.

<sup>2</sup>G. E. Hardy and J. K. Hulm, *Phys. Rev.* **93**, 1004 (1954).

<sup>3</sup>S. Geller and B. T. Matthias, *J. Am. Chem. Soc.* **77**, 1502 (1955).

<sup>4</sup>See the various articles in *Superconductivity in d- and f-Band Metals*, edited by D. H. Douglass (Plenum, New York, 1976).

<sup>5</sup>L. F. Mattheiss, *Phys. Rev. B* **12**, 2161 (1975).

<sup>6</sup>B. M. Klein and D. A. Papaconstantopoulos, in *Proceedings of the Conference on Low Lying Vibrational Modes*, San Juan, Puerto Rico, 1975 (unpublished).

<sup>7</sup>B. W. Roberts, *J. Phys. Chem. Ref. Data* **5**, 581 (1976).

<sup>8</sup>J. E. Graebner and J. E. Kunzler, *J. Low Temp. Phys.* **1**, 443 (1969).

<sup>9</sup>S. Berko and M. Weger, *Phys. Rev. Lett.* **24**, 55 (1970).

<sup>10</sup>H. Schäfer and W. Fuhr, *J. Less-Common Metals* **8**, 375 (1965).

<sup>11</sup>Z. Fisk and G. W. Webb, Phys. Rev. Lett. 36, 1084 (1976).

<sup>12</sup>R. W. Stark and L. R. Windmiller, Cryogenics 8, 872 (1968); A. J. Arko, M. B. Brodsky, G. W. Crabtree, D. Karim, D. D. Koelling, and L. R. Windmiller,

Phys. Rev. B 12, 4102 (1975).

<sup>13</sup>J. B. Ketterson (private communication).

<sup>14</sup>M. Weger and G. Barak, Phys. Lett. A 48, 319 (1974).

<sup>15</sup>T. Jarlborg and G. Arbman, J. Phys. F 6, 1976.